Desalination and Water Treatment
www.deswater.com
doi: 10.1080/19443994.2014.890548

54 (2015) 1850–1861
May

Taylor & Francis
Taylor & Francis Group

Adsorptive removal of 2,4-dinitrophenol using active carbon: kinetic and equilibrium modeling at solid–liquid interface

Krishnan Anoop Krishnan[a,*], Sivaseela Sini Suresh[a,b], Sasikumari Arya[a], Kumaran Girija Sreejalekshmi[c]

[a]*Chemical Sciences Division, National Centre for Earth Science Studies (NCESS), Ministry of Earth Sciences (MoES), Akkulam, Thuruvikkal Post 695031, Trivandrum, India*
Tel. +91 471 2511690; email: sreeanoop@rediffmail.com
[b]*Department of Chemistry, Sree Narayana College, Sivagiri, Varkala, Trivandrum, India*
[c]*Department of Chemistry, Department of Space, Indian Institute of Space Science and Technology (IIST), Near LPSC, Valiamala Post 695547, Trivandrum, India*

Received 12 October 2013; Accepted 27 January 2014

ABSTRACT

Adsorption is found to be a feasible technique for the removal of even trace amounts 2,4-dinitrophenol (2,4-DNP) from aqueous phase using active carbon from rubber wood. Prior to adsorption studies, surface and physical properties of active carbon were determined using X-RD, FT-IR, and particle size analyzer. Batch adsorption experiments were carried out to optimize various conditions, such as solution pH, contact time, initial solute concentration, and adsorbent dose, for the effective removal of 2,4-DNP from aqueous phase. The favorable pH range for the adsorption process was found to be 2.0–5.0. The maximum adsorption of 99.9% (24.98 mg/g), 98.2% (49.10 mg/g) and 96.9% (96.89 mg/g) of 2,4-DNP onto active carbon was observed at pH 4.0 for different initial concentrations of 50, 100, and 200 mg/L, respectively. Kinetics and isotherm studies showed that the adsorptive removal process follows pseudo-second-order kinetics and Langmuir isotherm, respectively.

Keywords: Adsorption; Active carbon; Wastewater treatment; Kinetic parameters; Phenol

1. Introduction

Among the phenolic compounds, nitrophenols are highly toxic to living organisms and create an oxygen demand in receiving waters. Most nitrophenols are resistant to biological treatment process because of the presence of nitro group in their structure providing them a strong chemical stability and resistance to microbial degradation. Nitrophenols and related compounds are released to the environment from pesticide and automobile exhaust gas or as a result of the photochemical reaction of benzene with nitrogen monoxide in highly polluted air and hence are found as contaminants in water, wastewaters and in the atmosphere [1]. In the phenolic family, 2,4-dinitrophenol (2,4-DNP) is considered to be the most toxic substance with an LD_{50} of 30 mg/kg body weight in rats [2] and is regulated as a priority pollutant by the Clean Water Act [3] which signifies developing efficient and low-

*Corresponding author.

cost strategies for the removal of 2,4-DNP from aqueous solution.

Many methods are reported for the removal of phenol and its nitro derivatives from water and wastewaters which include chemical oxidation [4,5], precipitation [6], solvent extraction [7], and adsorption [8,9]. Biological as well as chemical treatment of water and wastewater polluted with nitrophenols, especially 2,4-DNP, is a difficult process. Many aerobic and anaerobic experiments have been conducted to check the possibility of biodegrading 2,4-DNP in aqueous phase [10–13]. It was observed that 2,4-DNP is exploited as a source for carbon and nitrogen by large colonies of bacterial strains [14,15]. Apart from that, the highly complex process of biodegradation poses considerable challenge in the optimization and selection of favorable conditions. In the long run, the process seemed to be very difficult to implement and may also create excess sludge that requires disposal.

Adsorption process has proven to be efficient for the removal of phenolic compounds, and their derivatives from water and wastewaters using a plethora of adsorbents like Lakhra coal [16], zeolite [17], sludge [18], chitin [19], fly ash [20] and waste tires [21] and activated carbons [22]. Among these adsorbents, the high adsorption capabilities of activated carbons are attributed to their high surface area, pore volume, and porosity [23]. Adsorptive removal of 2,4-DNP from water and wastewaters using surface modified smectite clay [24] and molecular imprinted polymers [25] were proven to be effective. However, there is a wide scope of exploring the possibility of expanding the adsorbent materials based on activated carbon from saw dust which if accumulated may add harmful leachates into local water bodies. Further, the adsorption capacities of saw dust based activated carbon may vary with the source and such studies are very meagre in the literature, especially for the removal of 2,4-DNP.

Considering the above aspects, we have set a goal to provide viable adsorbent material from rubber wood saw dust for treating phenol embedded wastewaters, with a focus on 2,4-DNP removal, and to study the kinetic and equilibrium features involved in the process. The study involves the preparation of activated carbon from rubber wood active carbon from rubber wood (ACRW) and surface characterization of the adsorbent employing X-RD, FT-IR, and particle size analyzer. The effectiveness of ACRW as an adsorbent for the removal of 2,4-DNP will be studied by the optimization of various experimental conditions, such as solution pH, contact time, initial 2,4-DNP concentration, and adsorbent dose. The work also envisage to evaluate kinetic and equilibrium data using dynamic and isotherm models for assessing the order of adsorption process and adsorption capacity of carbon in removing 2,4-DNP from aqueous solutions, respectively.

2. Experimental procedure

2.1. Materials

All reagents were obtained from E. Merck India Ltd. Distilled water with a specific conductivity less than 1 μmho/cm was used throughout the study. Stock solutions of the test reagents (1,000 mg/L) were prepared by dissolving accurate amount of 2,4-DNP in Millipore water. All the required experimental solutions were prepared by diluting the stock solutions with Millipore water. ACRW was prepared from the rubber wood saw dust obtained from a local industry situated at Kodangavila, Trivandrum, Kerala, India was used as the adsorbent for the entire adsorption studies. Initially, the saw dust of rubber wood (25 g) was washed using distilled water repeatedly (10 times) to remove dirt and adhered particles and successively dried in natural sun light for over 10 h continuously. Then, it was kept in a muffle furnace maintained at 400˚C at a heating rate of 5˚C/min. The charring process completed at around 200˚C and the temperature reached 400˚C with in 75 min of time and was further kept at the same temperature up to 3 h. Fine droplets of distilled water (2 mL/min with an interval of 5 min) was purged in to the muffle furnace using specially made parallel inlet system (10 inlets in a row) without affecting the heating rate. The purging process was meant for increasing the porosity of the carbon. After the 3 h of heating process, the carbon (ACRW) was taken out (after cooling) and kept in an airtight polypropylene container and the same was used for adsorption experiments without any further process. Yield of the final product was 45.0% of the original material. The commercial activated carbon obtained from E. Merck India Ltd was used for comparative studies.

2.2. Analytical tools

The estimation of 2,4-DNP in supernatant solution was performed using UV–visible spectrophotometer (Shimadzu, model 1800). The pH measurements were made using a pH meter (Cyber pH-14 L) coupled with a combined electrode. X-ray diffraction patterns of active carbons (before and after adsorption) were recorded on powder X-ray diffractometer (Philips XPERT-PRO) with Cu Kα radiation (1.5406 Å)

employing X'celerator detector and monochromator at the diffracted beam side at 25°C (scan type: continuous, PSD mode: scanning, PSD length (°2θ): 2.12, tension: 40 kV and current: 30 mA). FT-IR spectra of the adsorbents were recorded between 4,000 and 400 cm^{-1} using the KBr method with a Perkin Elmer Spectrum 65 IR spectrophotometer. The surface area and particle size distribution were determined using CILAS particle size analyzer, France (model 1180, range: 0.04–2,500 m). Moisture content was also determined. Tap and bulk density of active carbons were also determined.

2.3. Adsorption experiments

The experimental solutions of different 2,4-DNP concentrations were prepared from a stock solution of 1,000 mg/L. Batch adsorption experiments were carried to study the extent of 2,4-DNP adsorption onto AC under varying conditions. The batch adsorption experiments were carried out by taking 50 mL of desired concentration of experimental solution together with 100 mg of the adsorbent followed by constant shaking after adjusting to a particular solution pH. The pH of the experimental solutions was adjusted using various concentrations of HCl and NaOH solutions. After equilibration, the supernatant liquids were filtered, and 2,4-DNP concentration was determined using UV–visible spectrophotometer by the following Eq. (1).

$$q = [(C_0 - C_A)V]/m \quad (1)$$

where q, the amount of 2,4-DNP adsorbed onto unit amount of adsorbent (mg/g); C_0 and C_A, initial and equilibrium solution concentration (mg/L), respectively; V, volume of aqueous phase (mL) and m, mass of the adsorbent (g).

The optimum pH for the adsorption process was confirmed by the following experiment. The effect of solution pH on 2,4-DNP adsorption was studied using their three initial concentrations (50, 100, and 200 mg/L) with 100 mg of ACRW. The pH of each sample was adjusted between 2.0 and 10.0 using different standard solutions (0.001, 0.01, 0.1, 0.5, 1.0, and 2.0 M) of HCl and NaOH. The pH-adjusted solutions were shaken for a contact time of 1 h at 25°C. The residual solute concentration of each sample was measured. Kinetic experiments were performed using different initial concentrations of 2,4-DNP (200, 250, 350, and 500 mg/L). The pH of the solution was adjusted to constant values. Supernatant solution was filtered at predetermined time intervals, and residual solute concentration was determined using spectrophotometer. From this, various kinetic parameters can be calculated using kinetic equation.

Adsorption isotherm experiments were performed using different initial concentrations of 2,4-DNP, ranging from 50 to 1,000 mg/L. The pH of the solution was kept at optimum value. The sample bottles were shaken continuously for 1 h time. Adsorbent loadings were calculated from the mass balance after initial and residual concentrations had been determined. The effect of adsorbent dose was determined by using different doses of ACRW (25, 50, 100, 150, and 200 mg) for the removal of 2,4-DNP from an aqueous solution of initial concentration 250 mg/L.

2.4. Column experiments

Continuous column adsorption studies were carried out to determine the effect of flow rate, inflow 2-DNP concentration, and adsorption capacity of ACRW. Column studies are important because effluents from industries are dynamic systems, which are flowing with respect to the gravitational force. The studies are intended to determine the adsorption behavior of 2,4-DNP onto ACRW from the breakthrough curves. A specially made cylindrical polyacrylic transparent column having desired dimensions (inner diameter/height = 4.0 cm/60 cm) was used in the column study. The column was uniformly packed with dried ACRW, and inlet of the column was supported by inert wire gauze stacked on an adaptor to prevent the loss of ACRW. The working solution of 2,4-DNP is taken in a double-walled polyacrylic tank of capacity 100.0 L. The working volume of the column was measured as 12.0 L/d. The column worked continuously for 8 d at 30°C and flushed out 96.0 L of aqueous solution containing 100 mg/L of 2,4-DNP species.

3. Results and discussion

3.1. Adsorbent characterization

The surface and physical properties of ACRW is given in Table 1. The XRD pattern of ACRW (before and after adsorption) is presented in Fig. 1(A) and (B). The difference in diffraction pattern of ACRW (before and after adsorption) may be the indication of 2,4-DNP uptake by the adsorbent material. X-ray diffraction pattern of the ACRW was characteristic by showing d-spacing value of 3.33 Å for 100% peak, which indicates the transformation of graphitic carbon with a degree of graphitization of nearly 99.9%. The strong peak at $2\theta = 20.99$ also indicates the higher degree of

Table 1
Surface characteristics of ACRW

No.	Parameters	
1	Specific surface area (m^2/g)	2.15
2	Particle mean diameter (μm)	35.35
3	Total acidic sites (meq/g)	3.04
4	C (%)	92.9
5	H (%)	0.75
6	N (%)	0.32
7	O (%)	5.89
8	Ash content (%)	5.21
9	Moisture content (%)	4.92
10	Pore density (g/mL)	0.97
11	Tap density (g/mL)	2.82
12	Carboxylic acid content (meq/g)	1.62

graphitization. The other XRD peaks at day values of 2.44, 1.81, 1.54, 1.37, and 1.28 Å also confirm the presence of graphitic phase. But after the adsorption process, the number of peaks in the XRD pattern was decreased and the intensity is found to be slightly increased in most of the strong peaks. Thus, it clearly confirmed the feasibility of adsorption of 2,4-DNP onto ACRW. But the intensity of peaks correspond to $2\theta =$ 36.67 and 50.36 of ACRW is considerably reduced after the process of adsorption. Moreover, the strong peaks at $2\theta = 68.32$ and 73.69 are not found in the ACRW after the adsorption process.

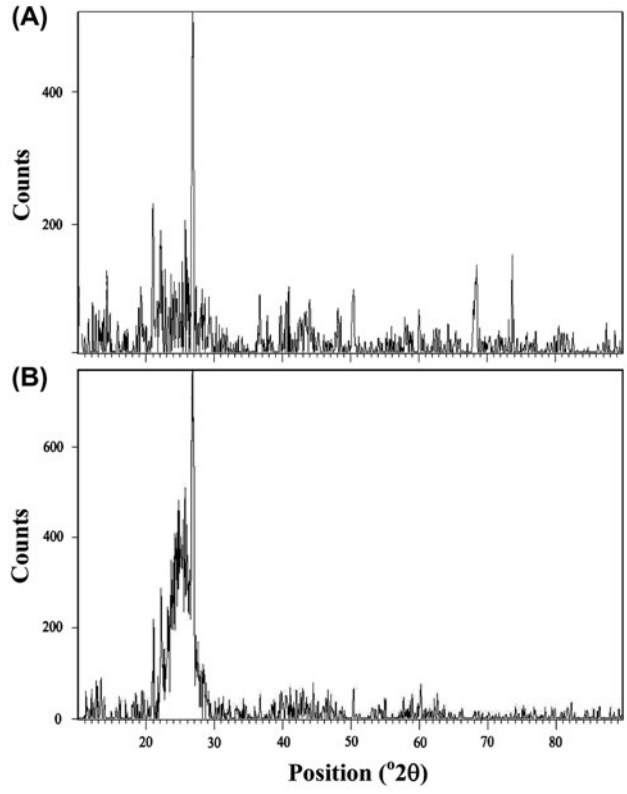

Fig. 1. X-RD spectra of ACRW (A) before adsorption, (B) after adsorption.

The FT-IR spectrum of ACRW before adsorption (ACRW-BA) and after adsorption (ACRW-AA) is shown in Figs. 2 and 3. In the case of ACRW-BA, the absorption peaks at 3,702 and 3,406 cm^{-1} corresponds to exchangeable O–H group stretching vibration. The IR spectrum shows bands at 2,926 and 2,853 cm^{-1} indicating the presence of C=C–H stretching vibrations. The absorption peak at 1,580 cm^{-1} corresponds to the C=O

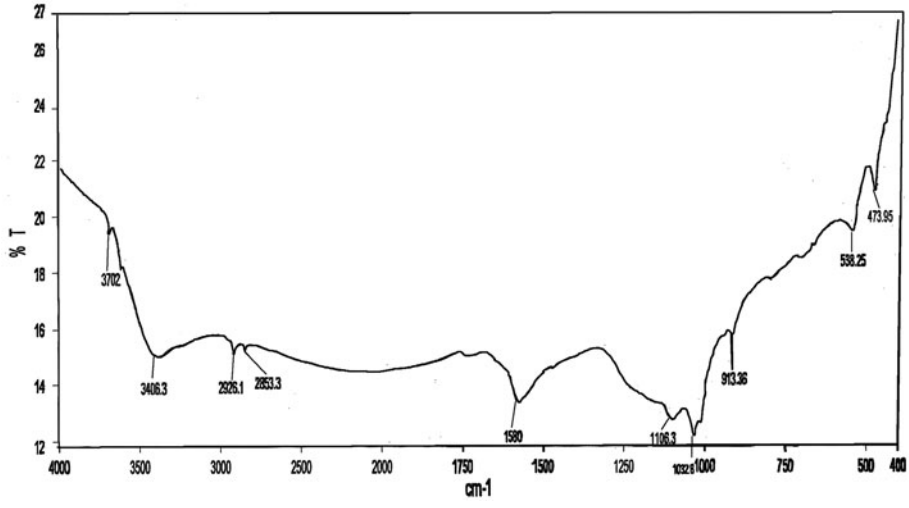

Fig. 2. FT-IR spectra of ACRW (before adsorption).

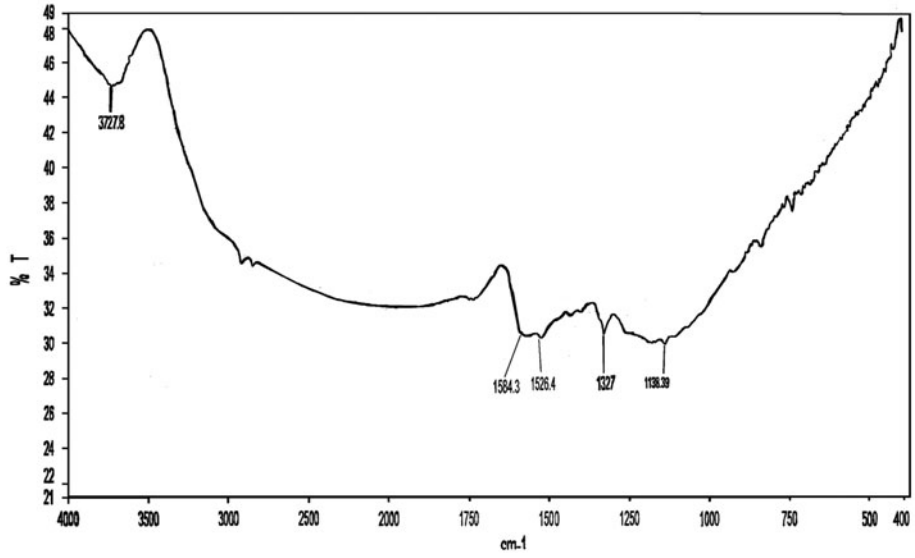

Fig. 3. FT-IR spectra of ACRW (after adsorption).

stretching of carbonyl group. The peak at 1,106 cm^{-1} may be due to the alcohol C–O stretching vibration. But in the case of ACRW-AA, it is very clear from the spectra that the band intensity of the carbonyl group has diminished and shifted as compared with ACRW-BA. Moreover, the number of bands in the finger print region of ACRW-AA has decreased with respect to those in ACRW-BA. In Fig. 3, bands at 3,727 cm^{-1} arises from hydroxyl stretching vibration. The bands at 1,584 cm^{-1} are assigned to the stretching vibration of carbonyl group. The peaks at 1,526 and 1,327 cm^{-1} indicates the N=O asymmetric and symmetric vibrations, respectively. These bands clearly confirmed the adsorption of 2,4-DNP onto the surface of ACRW.

3.2. Effect of solution pH

The removal of 2,4-DNP from aqueous solution by adsorption phenomenon is strongly dependent on the pH of the solution, which affects the surface charge of the adsorbent and speciation of the adsorbate. The effect pH on the adsorption process was studied over a wide range of pH from 2.0 to 10.0. The influence of pH on the adsorption of 2,4-DNP is shown in Fig. 4(A). From the figure, it is clear that the adsorptive removal of 2,4-DNP favorably occurred over the pH range 2.0–5.0. Above the pH range, minimum amount of adsorption is taking place. The maximum adsorption of 99.9% (24.98 mg/g), 99.9% (49.10 mg/g), and 96.9% (96.89 mg/g) of 2,4-DNP onto ACRW was observed at pH 4.0 for different initial concentrations of 50, 100, and 200 mg/L, respectively. The mechanism

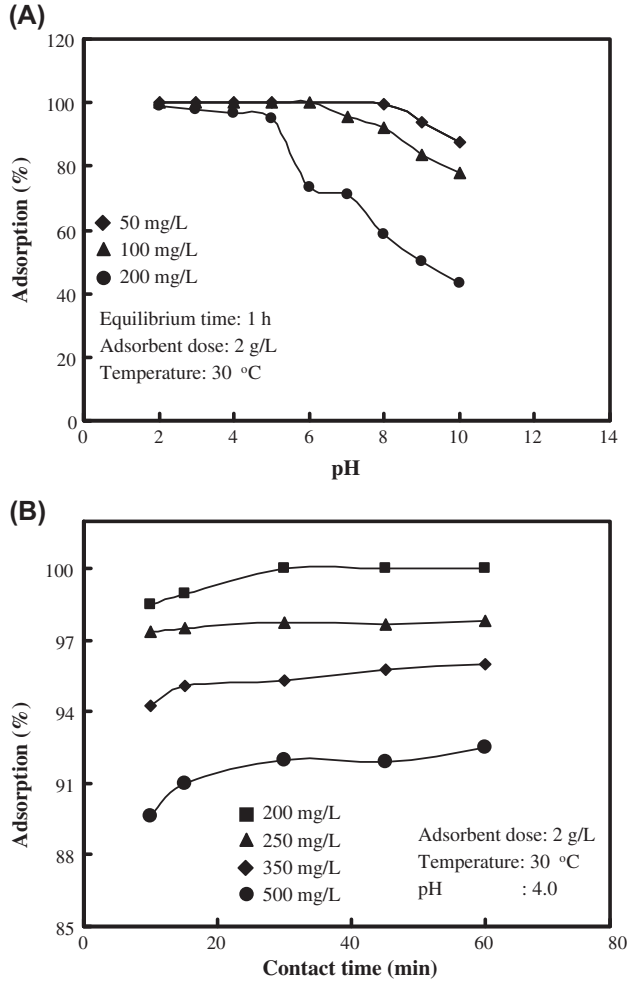

Fig. 4. Effect of (A) pH and (B) contact time on the adsorption of 2,4-DNP onto ACRW.

behind the adsorption process can be explained as follows. At lower pH values, hydrogen ion concentration is high and thereby the solid surface gets protonated. At the same time, phenoxide ion is formed due to ionization in aqueous phase. Therefore, the adsorption of 2,4-DNP onto ACRW at lower pH values taking place by the interaction of positively charged solid surface with the ionized form of phenolic group of 2,4-DNP.

The mechanism can be summarized as follows:

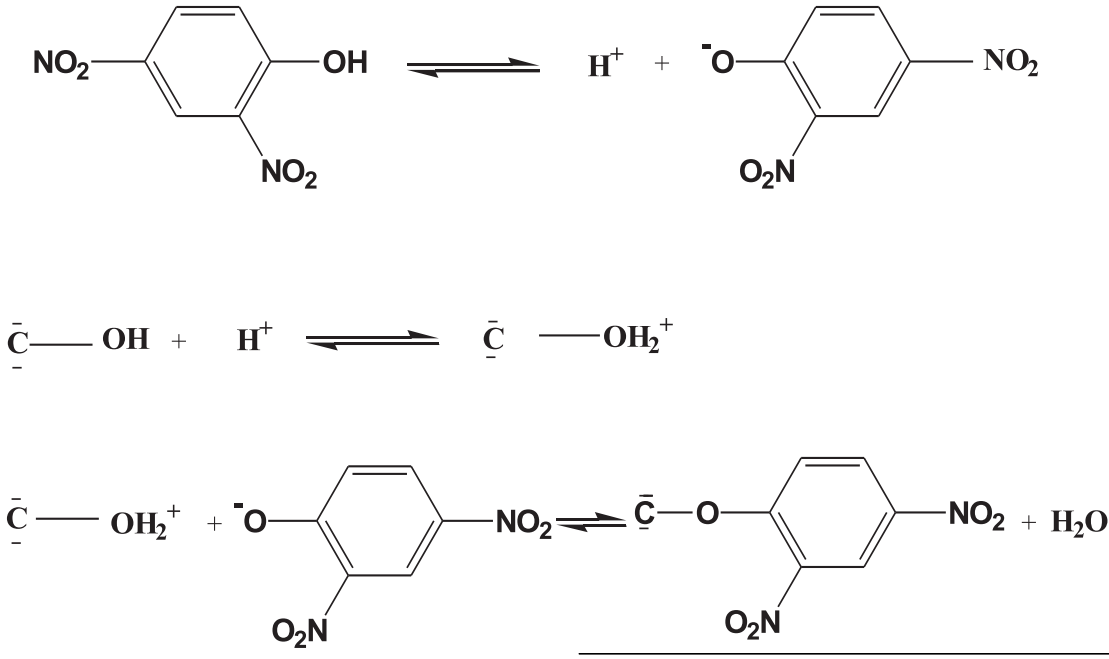

$\bar{C}$ indicates the adsorbent surface

3.3. Effect of initial concentration and contact time

Adsorptive removal of 2,4-DNP onto ACRW was carried out over a wide range of initial concentrations (200–500 mg/L) and at predetermined contact time varying from 0 to 1 h (Fig. 4(B)). From the figure, it is clear that the amount of adsorption increased with increase in 2,4-DNP initial concentration; however, the percentage adsorption is found to be decreased. At higher initial concentrations, the ratio of the initial number of moles of 2,4-DNP to the available adsorption sites is high; hence, the fractional adsorption becomes dependent on initial concentration. But the time required for attaining the equilibrium state is highly independent on initial concentration. The quantity of 2,4-DNP adsorbed onto ACRW increased with the contact time increase and attained equilibrium at 1 h. The amount of 2,4-DNP adsorption onto activated carbon is increased from 96.89 to 211.50 mg/g as the initial concentration increased from 200 to 500 mg/L at a contact time of 1 h. At the same time, the percentage of adsorption decreased from 96.9 to 84.6% as the initial concentration increased from 200 to 500 mg/L.

3.4. Adsorption kinetics

Adsorption kinetics and equilibria are the important physicochemical studies for the evaluation of basic characteristics of a good adsorbent. Kinetic as well as equilibrium data were used for assigning the appropriate models for explaining the nature of adsorption phenomenon. The amount of 2,4-DNP adsorbed at different time intervals for different initial concentrations varying from 200 to 500 mg/L is depicted in Fig. 4(B). From the figure, it is clear that 1 h time was presumed to represent the equilibrium time for the adsorption of 2,4-DNP onto ACRW at different initial concentrations. Two adsorption kinetic models used in this study are pseudo-first-order and pseudo-second-order equations developed by Lagergren [26] and Ho and McKay [27], respectively. The Lagergren pseudo-first-order is given by the Eq. (2):

$$\log\,(q_e - q_t) = \log\,q_e - \frac{k_1 t}{2.303} \tag{2}$$

where k_1 is the rate constant of pseudo-first-order adsorption and q_e and q_t represents the amount of 2,4-DNP adsorption at equilibrium and at time t,

respectively. The pseudo-second-order is given by the Eq. (3):

$$\frac{t}{q_t} = \frac{1}{k_2 q_e^2} + \frac{t}{q_e} \tag{3}$$

where q_e and q_t are the amount of 2,4-DNP adsorbed (mg/g) at equilibrium and at time t, respectively. The product $k_2 q_e^2$ is the initial sorption rate, represented as $h = k_2 q_e^2$. Kinetic parameters of these models were calculated from the slope and intercept of the linear plots of log $(q_e - q_t)$ vs. t Fig. 5(A) and t/q_t vs. t Fig. 5(B). The kinetic parameters are given in Table 2 The values of k_1 and k_2 were found to be greater for an initial concentration of 200 mg/L and decreases gradually as the initial concentration increases to 500 mg/L for the adsorption of 2,4-DNP onto ACRW. The values of rate constant k_1 increase from 0.0051 to 0.0588 /min, as the initial concentration increases from 200 to 500 mg/L for the adsorption of 2,4-DNP onto ACRW. Similarly, the values of k_2 were found to decrease from 0.0472 to 0.0154 g/mg min, as the initial concentration increases from 200 to 500 mg/L. In pseudo-second-order kinetic model, the values of h increase with increase in initial concentration. The h values are depicted in Table 2.

To compare the validity of each model, a normalized standard deviation, Δq (%) was calculated using the following Eq. (4).

$$\Delta q\ (\%) = 100 \times \sqrt{\frac{\sum[(q_t^{exp} - q_t^{cal})/q_t^{exp}]^2}{N-1}} \tag{4}$$

where q_t^{exp} and q_t^{cal} are experimental and calculated amount of 2,4-DNP adsorbed on ACRW at time t and N is the number of measurements made. Table 2 presents the values of Δq (%) and correlation coefficients (r^2). The value of Δq (%) for pseudo-second-order kinetic model is very low compared with that for pseudo-first-order kinetic model. The values of correlation coefficients for the adsorption of 2,4-DNP onto ACRW from all the systems were found to be 0.99 for pseudo-second-order kinetic model and 0.51–0.95 for pseudo-first-order kinetic model. Based on correlation coefficients and Δq (%) values, it is evident that the adsorption of ACRW can be best explained using the pseudo-second-order kinetic model.

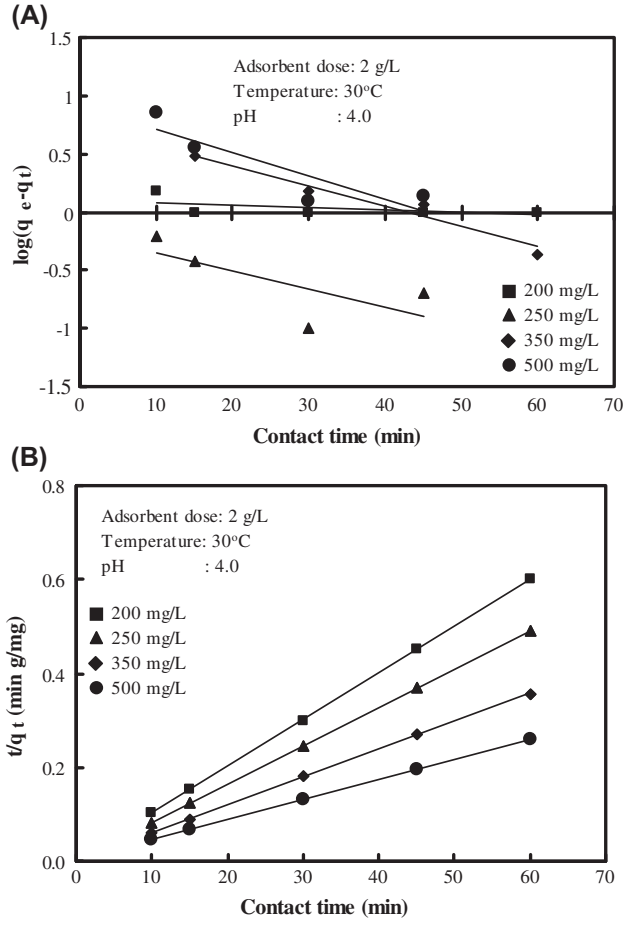

Fig. 5. (A) Pseudo-first-order, (B) pseudo-second-order kinetic plots for the adsorption of 2,4-DNP onto ACRW.

The adsorption mechanism could be controlled either by reaction kinetics or by diffusion process (film diffusion or pore diffusion). In the present study, due to constant agitation, the shear on the particle surface is high. Therefore, the thickness of the boundary layer surrounding the particles should be minimal. In order

Table 2
Kinetic parameters for the adsorption of 2,4-DNP onto ACRW

	Pseudo-first-order			Pseudo-second-order			
C_o (mg/L)	k_1 (min^{-1})	r^2	Δq (%)	k_2 (g/mg min)	h (mg/g min)	r^2	Δq (%)
200	0.0051	0.507	21.14	0.0588	588.24	0.997	2.92
250	0.0355	0.450	18.23	0.0420	625.00	0.998	2.17
350	0.0403	0.789	13.70	0.0249	714.29	0.996	3.71
500	0.0472	0.954	7.59	0.0154	833.33	0.997	2.46

Table 3
Film and pore diffusion coefficients for the adsorption of 2,4-DNP onto ACRW

C_o (mg/L)	$t_{1/2}$ (s)	D_f (cm^2/s)	D_p (cm^2/s)
200	120	1.47×10^{-6}	5.76×10^{-9}
250	150	5.96×10^{-7}	5.68×10^{-9}
350	180	3.91×10^{-7}	5.34×10^{-9}
500	240	1.45×10^{-7}	2.89×10^{-9}

to assess the nature of the diffusion process responsible for the adsorption of 2,4-DNP onto ACRW, attempts were made to calculate coefficients of the process. Assuming spherical geometry for the carbons, film diffusion (D_f) and pore diffusion (D_p) coefficients were calculated [28] using the following Eqs. (5) and (6).

$$D_f = 0.23 \times \frac{r_0 \delta}{t_{1/2}} \times \frac{\overline{C}}{C} \quad (5)$$

$$D_p = 0.03 \times \frac{r_0^2}{t_{1/2}} \quad (6)$$

where r_0 is the radius of the adsorbent particle (4.8×10^{-3} cm), δ is the film thickness (1×10^{-3} cm) [29], $\overline{C}/C$ is the equilibrium loading of the adsorbent and $t_{1/2}$ is the time required for half adsorption. According to previous report [30] for film diffusion to be rate limiting, the values of D_f should be in the range of 10^{-6}–10^{-8} cm^2/s. For pore diffusion to be rate limiting, the value of D_p should be in the range of 10^{-11}–10^{-13} cm^2/s. The kinetic data (q_t vs. t) obtained for different initial concentrations were used to calculate diffusion coefficients for the adsorption of 2,4-DNP onto ACRW. The results are present in Table 3. It is evident that the rate-limiting step appears to be film diffusion process since the coefficient values are in the order of 10^{-6}–10^{-7} cm^2/s. The values of both D_f and D_p decreased with increasing initial concentration of 2,4-DNP. A similar variation in D_f and D_p with increasing concentration was also observed for the removal of fluoride on iron(III)/zirconium(IV) hybrid oxide [31].

3.5. Adsorption isotherms

Equilibrium isotherms relate to the amount of solute adsorbed onto surface of solid to that of the concentration of solute in aqueous phase at equilibrium. The study of isotherms is highly needed to find out the effectiveness of the adsorbent material for the removal of solutes from aqueous solutions. Moreover, it is helpful in designing and optimizing an adsorption system for the removal process [32]. Equilibrium studies were performed for the adsorption of 2,4-DNP onto ACRW at pH 4.0 for various initial concentrations of 2,4-DNP ranging from 50 to 1,000 mg/L. From the experimental results, it is obvious that as the initial concentration increases the amount of adsorption also increases. The equilibrium data obtained from adsorption studies were applied to Langmuir [33] and Freundlich isotherm model [34] and can be represented by the following Eqs. (7) and (8).

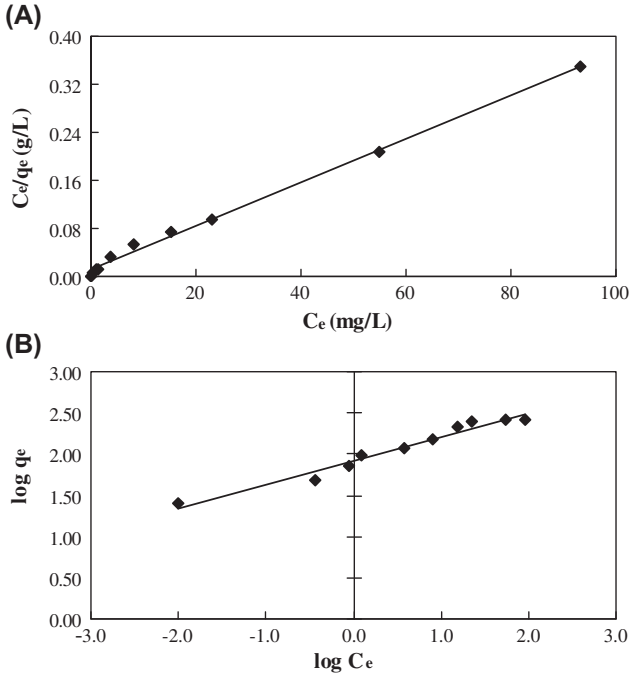

Fig. 6. Langmuir (A) and Freundlich (B) isotherm plots for the adsorption of 2,4-DNP onto ACRW.

$$\frac{C_e}{q_e} = \frac{1}{Q^0 b} + \frac{C_e}{Q^0} \quad (7)$$

$$\log q_e = \log K_F + \frac{1}{n} \log C_e \quad (8)$$

where q_e is the amount of 2,4-DNP adsorbed per unit weight of active carbon in mg/g, C_e is the equilibrium solution concentration in mg/L. Q^0 and b are the Langmuir constants related to the adsorption capacity (mg/g) and energy of adsorption (L/mg). K_F and $1/n$ are Freundlich constants related to adsorption capacity and energy of adsorption respectively. The isotherm plots drew using the Eqs. (7) and (8) are depicted in Fig. 6. From the plots, it is confirmed that the value of r^2 for Langmuir isotherm is lower than that of Freund-

Table 4
Langmuir and Freundlich isotherm constants for the adsorption of 2,4-DNP onto ACRW

Langmuir isotherm			Freundlich isotherm		
Q^0 (mg/g)	b (L/mg)	r^2	K_F (mg/g)	$1/n$ (L/mg)	r^2
277.78	0.1186	0.997	83.50	0.2869	0.972

lich isotherm, and therefore, the later one is the best fit model for explaining the adsorption of methylene blue onto china clay. The values of Q^0, b, K_F and 1/n are presented in Table 4.

The applicability of the Langmuir isotherm can be articulated by the equilibrium parameter, R_L [35] and can be represented by the following Eq. (9).

$$R_L = \frac{1}{(1 + bC_o)} \tag{9}$$

where b and C_o are same as in the Langmuir isotherm model and represents the Langmuir constant and initial concentration of 2,4-DNP solution, respectively. R_L values indicate the feasibility of adsorption process. The favorable adsorption process is indicated by the values of R_L in the order $0 < R_L < 1$. From the experimental data, the values of R_L were found to be between 0 and 1 for all initial concentrations of 2,4-DNP varying from 50 to 1,000 mg/L and there by obeying the Langmuir isotherm model (Table 5).

The best suited isotherm model among Langmuir and Freundlich isotherms was confirmed from the values of normalized standard deviation Δq (%), which was calculated using the Eq. (4). The Δq (%) values are presented in Table 4 along with correlation coefficients (r^2). The lowest values of Δq (%) for Langmuir isotherm model confirms its fitness in explaining the equilibrium data for the adsorption of 2,4-DNP onto ACRW. The correlation coefficient values for the adsorption of 2,4-DNP onto ACRW from all the experimental set up were found to be 0.99 for Langmuir model and 0.95–0.98 for Freundlich model. Based on correlation coefficients and Δq (%) values, it is evident that the adsorption of 2,4-DNP can be best described by Langmuir isotherm model. The theoretically calculated amount of 2,4-DNP adsorbed onto ACRW using Langmuir and Freundlich isotherm models for different initial concentrations (50–1,000 mg/L) was compared with the experimental equilibrium data and shown in Fig. 7(A) and in turn confirms the fitness of the former isotherm model in explaining the adsorption of 2,4-DNP onto ACRW.

Table 5
R_L values for the adsorption of 2,4-DNP onto ACRW

Initial concentration (mg/L)	R_L value
50	0.0591
100	0.0304
150	0.0205
200	0.0155
250	0.0124
350	0.0089
500	0.0062
600	0.0052
800	0.0039
1,000	0.0031

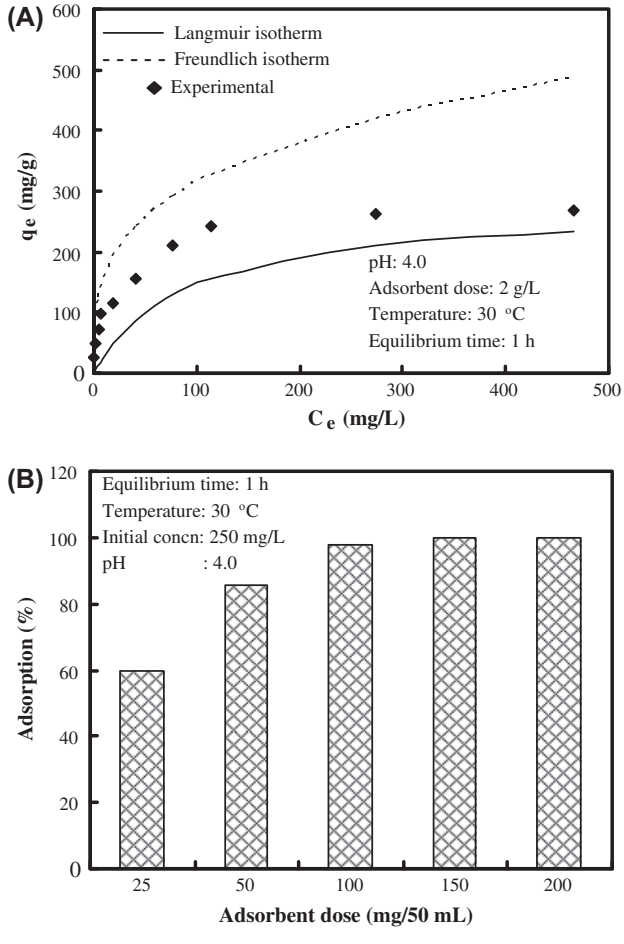

Fig. 7. (A) Plots of q_e vs. C_e on the adsorption of 2,4-DNP on to ACRW, (B) effect of ACRW dose on the removal of 2,4-DNP from aqueous solution.

Thermodynamic parameters such as change in free energy (ΔG°), enthalpy (ΔH°), and entropy (ΔS°) were also calculated using the following equation.

$$\Delta G^\circ = -\mathrm{RT}\ln K_0 \quad (10)$$

$$\ln K_0 = \frac{\Delta S^\circ}{R} - \frac{\Delta H^\circ}{\mathrm{RT}} \quad (11)$$

where K_0 represents equilibrium constant. The values of K_0 were determined from the intercepts obtained by plotting ln q_e/C_e vs. q_e (figure not shown) as suggested by Khan and Singh [36] and extrapolating to zero q_e at various temperatures ranging from 30 to 60°C. The values of K_0 were found to be 6.49, 8.29, 8.90, and 8.98 for 30, 40, 50, and 60°C, respectively. The plots of ln K_0 vs. 1/T for 2,4-DNP adsorption onto ACRW was found to be linear (figure not shown). The values of ΔH° and ΔS° were obtained from the slope and intercept of the plots and were 8.60 kJ mol^{-1} and 44.43 J mol^{-1} K^{-1}, respectively. The positive value of ΔH° indicates that the adsorption of 2,4-DNP onto ACRW is endothermic in nature. The values of ΔG° were found to be −4.71, −5.50, −5.87, and −6.08 kJ mol^{-1} for the adsorption of 2,4-DNP from aqueous solution at 30, 40, 50, and 60°C, respectively. The negative values of ΔG° demonstrate the spontaneity of adsorption process. The value of ΔG° decreases with increasing temperature, showing an increase in the adsorption feasibility at higher temperatures. The positive value of ΔS° suggested some structural changes in adsorbent and adsorbate and also reflects the affinity of ACRW under consideration towards 2,4-DNP molecules.

3.6. Effect of adsorbent dose

The effect of adsorbent dose on 2,4-DNP adsorption is shown in Fig. 7(B). From the figure, it is clear that the percentage removal increased with increasing adsorbent concentration. This may be attributed to the greater availability of adsorption sites or surface area at higher concentrations of the adsorbent. The effect of adsorbent dose (25–200 mg/50 mL) for the adsorptive removal of 2,4-DNP from aqueous solutions of initial concentrations 250 mg/L has been tested at pH 4.0. For initial concentration 250 mg/L, a minimum of 150 mg/50 mL of ACRW was required for the complete removal of 2,4-DNP from aqueous solutions.

3.7. Continuous column studies

The experimental solution of 2,4-DNP having initial concentration 100 mg/L was introduced into the polyacrylic column (upward flow method) at a fixed rate of 8.33 mL/min using peristaltic pump from the polyacrylic tank. Retention time was found to be 1.4 h. The effluent from the outlet of the column was analyzed for 2,4-DNP concentration at regular intervals. The adsorption column was operated for 8 d, and subsequently, a breakthrough curve was determined. From the breakthrough curve (Fig. 8), the adsorption capacity of ACRW was found to be 285.41 mg/g, which is in good agreement with the adsorption capacity calculated using batch adsorption experiment.

3.8. Desorption and regeneration studies

The regeneration of the spent ACRW for the successive removal of 2,4-DNP from aqueous phase is very important for evaluating the feasibility of the adsorption process in real practices. This can be carried out by desorbing the adsorbed 2,4-DNP from the spent ACRW using extracting mediums such as dilute mineral acids or bases and also using dilute salt solutions. Among the mediums used, 0.01 M NaOH was found to be good enough for desorbing the adsorbed 2,4-DNP from the spent adsorbent. The ACRW loaded with the maximum amount of 2,4-DNP were placed into desorbing medium containing 0.01 M NaOH and the amount of 2,4-DNP desorbed was measured at 4 h of contact time. Table 6 shows the results of the adsorption and desorption of 2,4-DNP onto ACRW for an initial concentration of 100 mg/L. It can be seen that bound 2,4-DNP is quantitatively desorbed from the ACRW surface to the suspending medium (>95%) in the first cycle. The second, third, and fourth adsorption cycles reveal that ACRW can be reused with very small loss

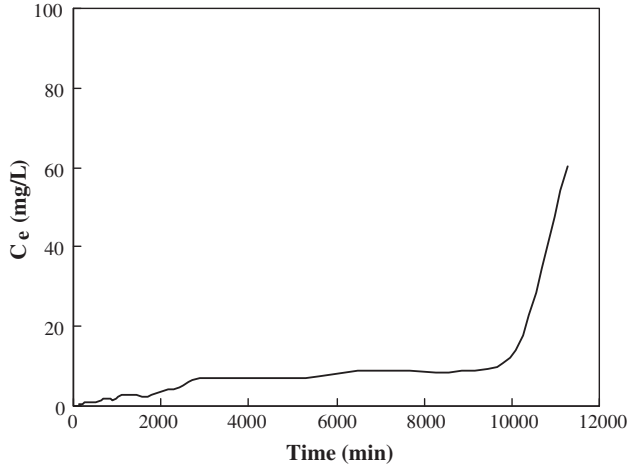

Fig. 8. Breakthrough curve for the adsorption of 2,4-DNP onto ACRW.

Table 6
Desorption and regeneration data for 2,4-DNP onto ACRW[a]

Cycle	Adsorption (mg/g)	Desorption at 0.01 M NaOH (mg/g)
1	49.10 (98.2)	48.36
2	48.35 (96.7)	47.82
3	47.75 (95.5)	45.28
4	46.10 (92.2)	44.21

[a]Values shown in the parenthesis are in percent.

in efficiency. Approximately, 88.7% of the initial desorption capacity is obtained in the fourth cycle.

4. Conclusion

We have successfully employed ACRW for the effective removal of 2,4-DNP using batch adsorption technique. The adsorption of 2,4-DNP was found to be strongly dependent on the pH of the solution, initial 2,4-DNP concentration, and contact time. The maximum adsorption was found to be in the pH range of 2.0–5.0 and maximum value obtained at pH 4.0. We have put forth a mechanism for 2,4-DNP adsorption at the solid/liquid interface. For an initial concentration of 50 mg/L at pH 4.0, a maximum of 99.9% (24.98 mg/g) of 2,4-DNP was adsorbed onto ACRW. Kinetic data follow a pseudo-second-order equation, while isotherm data follow Langmuir equation. The adsorption capacity was found to be 277.78 mg/g. Encouraged by the results, we are widening our studies to evaluate the potential of sawdust-based activated carbon from different sources for the adsorptive removal of nitrophenols, and the results will be summarily published.

Acknowledgments

The authors are thankful to the Director of NCESS, Dr N.P. Kurian for providing the laboratory and knowledge resource facilities. We also thank the national program COMAPS (Coastal Ocean Monitoring and Prediction System) funded by MoES (Ministry of Earth Sciences), Government of India for extending their working facilities. The work was initiated as part of the PG Studentship Program of NCESS and is greatly acknowledged. The facilities provided by the X-ray Diffraction Laboratory and Particle Size Analyser Lab of NCESS are also greatly acknowledged. The authors also thank the Department of Chemistry, University College, Palayam, Trivandrum for providing the FT-IR spectra.

References

[1] C. Leuenberger, J. Czuczwa, J. Tremp, W. Giger, Nitrated phenols in rain: Atmospheric occurrence of phytoxic pollutants, Chemosphere 17 (1998) 511–515.
[2] J. Shea, J. Weber, M. Overcash, Biological activities of 2, 4-dinitrophenol in plant–soil systems, Residue Rev. 87 (1983) 1–41.
[3] US Environmental Protection Agency, Water-related Environmental Fate of 129 Priority Pollutants: Volume II: Office of Water Planning and Standards, Office of Water and Waste Management, US Environmental protection agency, Washington, DC, 1979.
[4] P. Kumar, H. Nikakhtari, M. Nemati, G.A. Hill, Oxidation of phenol in a bioremediation medium using Fenton's reagent, Environ. Technol. 31 (2010) 47–52.
[5] D. Manojlovic, D.R. Ostojic, B.M. Obradovic, M.M. Kuraica, V.D. Krsmanovic, J. Puric, Removal of phenol and chlorophenols from water by new ozone generator, Desalination 213 (2007) 116–122.
[6] X. Xian, P. He, J. Jin, Z. Ho, Study on Us/O_3 mechanism in pentachlorophenol decomposition, J. Zhejiang Univ. Sci. 6 (2005) 569–573.
[7] Y. Parka, A.H.P. Skelland, L.J. Forney, J.H. Kim, Removal of phenol and substituted phenols by newly developed emulsion liquid membrane process, Water Res. 40 (2006) 1763–1772.
[8] S.R. Ha, S. Vinitnantharat, Competitive removal of phenol and 2,4-dichlorophenol in biological activated carbon system, Environ. Technol. 21 (2000) 387–396.
[9] S.H. Lin, M.J. Cheng, Phenol and chlorophenol removal from aqueous solution by organobentonites, Environ. Technol. 21 (2000) 475–482.
[10] L. Virginia, A. Gemini, T. Valeria, C. Daniel, P. Estela, K. Sonia, Microbial degradation and detoxification of 2,4-dinitrophenol in aerobic and anoxic processes, Int. Biodeter. Biodegr. 60 (2007) 226–230.
[11] S. Zonglian, G. Mengchun, J. Chunji, C. Youyuan, Y. Jianwei, Toxicity and biodegradation of 2,4-dinitrophenol and 3-nitrophenol in anaerobic systems, Process Biochem. 40 (2005) 3017–3024.
[12] M. Haghighi-Podeh, S. Bhattacharya, Fate and toxic effects of nitrophenols on anaerobic treatment systems, Water Sci. Technol. 34 (1996) 345–350.
[13] L. Krumholz, J. Suflita, Anaerobic aquifer transformations of 2,4- dinitrophenol under different terminal electron accepting conditions, Anaerobe. 3 (1997) 399–403.
[14] S. Ebert, P. Rieger, H. Knackmuss, Function of coenzyme F420 in aerobic catabolism of 2,4,6-trinitrophenol and 2, 4-dinitrophenol by Nocardioides simplex FJ2–1A, J. Bacteriol. 181 (1999) 2669–2674.
[15] R. Blasco, E. Moore, V. Wray, D. Pieper, K. Timmis, F. Castillo, 3-Nitroadipate, a metabolic intermediate for mineralization of 2,4-dinitrophenol by a new strain of a Rhodococcus species, J. Bacteriol. 181 (1999) 149–152.
[16] M. Ishaq, I. Ahmad, M. Shakirullah, H. Ur Rehman, M.A. Khan, I. Ahmad, I. Ur Rehman, Adsorption study of phenol on Lakhra coal, Toxicol. Environ. Chem. 89 (2007) 1–6.
[17] C. Díaz-nava, M.T. Olguin, M. Solache-ríos, M.T. Alarcon-herrera, A. Aguilar-Elguezabal, Effects of

preparation and experimental conditions on removal of phenol by surfactant-modified zeolites, Environ. Technol. 29 (2008) 1229–1239.
[18] C.S. Arslan, A.Y. Dursun, Biosorption of phenol on dried activated sludge: Effect of temperature, Sep. Sci. Technol. 43 (2008) 3251–3268.
[19] A. Dursun, C. Kalayci, Equilibrium, kinetic and thermodynamic studies on the adsorption of phenol onto chitin, J. Hazard. Mater. B123 (2005) 151–157.
[20] S.O. Bada, J.H. Potgieter, A.S. Afolabi, Kinetics studies of adsorption and desorption of south african fly ash for some phenolic compounds, Particul. Sci. Technol. 31 (2013) 1–9.
[21] W. Tanthapanichakoon, P. Ariyadejwanich, P. Japthong, K. Nakagawa, S. Mukai, H. Tamon, Adsorption–desorption characteristics of phenol and reactive dyes from aqueous solution on mesoporous activated carbon prepared from waste tires, Water Res. 39 (2005) 1347–1353.
[22] C. Hua, R. Zhang, L. Li, X. Zheng, Adsorption of phenol from aqueous solutions using activated carbon prepared from crofton weed, Desalin. Water Treat. 37 (2012) 230–237.
[23] M. Ahmaruzzaman, Adsorption of phenolic compounds on low-cost adsorbents: A review, Adv. Colloid Interfac. 143 (2008) 48–67.
[24] V.K. Tchieda, I.K. Tonle, M.C. Tertis, E. Ngameni, M. Jitaru, Adsorption of 2,4-DNP and 2,6-dinitrophenol onto organoclays and inorganic-organic pillared clays, Environ. Eng. Manage. J. 9 (2010) 953–960.
[25] N.D. Zakaria, N.A. Yusof, J. Haron, A.H. Abdullah, Synthesis and evaluation of a molecularly imprinted polymer for 2,4-DNP, Int. J. Mol. Sci. 10 (2009) 354–365.
[26] S.K. Lagergren, About the theory of so-called adsorption of soluble substances, Kungliga Svenska Vetenskapsakademens Handlingar 24 (1898) 1–39.
[27] Y.S. Ho, G. McKay, The kinetics of sorption of divalent metal ions onto sphagnum moss peat, Water Res. 34 (2000) 735–742.
[28] A.K. Battacharya, C. Venkobacher, Removal of cadmium(II) by low cost adsorbents, J. Environ. Eng. 110 (1984) 110–115.
[29] F. Helfferich, Ion exchange,McGraw-Hill, New York, NY, 1962.
[30] L.D. Michelson, P.G. Gideon, E.G. Pace, L.H. Kntel, Removal of soluble mercury from wastewater by complexing techniques, US Department of Industry, Office of Water Research and Technology, Bull. No. 74 (1975).
[31] K. Biswas, D. Bandhoyapadhyay, U.C. Ghosh, Adsorption kinetics of fluoride on iron(III)-zirconium (IV)hybrid oxide, Adsorption 13 (2007) 83–94.
[32] B. Benguella, H. Benaissa, Cadmium removal from aqueous solution by chitin: Kinetic and equilibrium studies, Water Res. 36 (2002) 2463–2474.
[33] I. Langmuir, The adsorption of gases on plane surface of glass, mica and platinum, J. Am. Chem. Soc. 40 (1918) 1361–1403.
[34] H.M.F. Freundlich, Over the adsorption in solution, J. Phys. Chem. 57 (1906) 385–470.
[35] G. McKay, H.S. Blair, J.R. Gardner, Two resistance mass transport model for the adsorption of acid dye onto chitin in fixed beds, J. Appl. Polym. Sci. 33 (1987) 1249–1257.
[36] A.A. Khan, R.P. Singh, Adsorption thermodynamics of carbofuran on Sn(IV) arsenosilicate in H^+, Na^+ and Ca^{2+} forms, Colloids Surf. 24 (1987) 33–42.